Proceedings of the Forty Second National Conference on Fluid Mechanics and Fluid Power

December 14-16, 2015, NITK Surathkal, Karnataka, India

FMFP 2015 – PAPER NO. 115

Numerical Investigations on the Effects of Transient Heat Input and Loading Conditions on the Performance of a Single-phase Closed-loop Thermo-syphon

Basim Freegah
School of Computing & Engineering
University of Huddersfield
Huddersfield, HD1 3DH, UK
Al-Mustansiriya University, Iraq
u1169570@hud.ac.uk

Taimoor Asim
School of Computing & Engineering
University of Huddersfield
Huddersfield, HD1 3DH, UK
t.asim@hud.ac.uk

Rakesh Mishra
School of Computing & Engineering
University of Huddersfield
Huddersfield, HD1 3DH, UK
r.mishra@hud.ac.uk

Karina Zala
School of Computing & Engineering
University of Huddersfield
Huddersfield, HD1 3DH, UK
karina.zala@hud.ac.uk

ABSTRACT

One of the most important sources of renewable energy is solar energy, which is readily available throughout the world. There is a requirement to make the solar energy affordable for everyday use in order to minimise the present reliance on fossil fuels. This would also assist in meeting the requirements of limiting greenhouse-gas effects, and hence conserve the environment from pollution, global warming, ozone layer depletion, etc. Thermo-syphons are systems that capture solar energy using a working fluid. In the present study, Computational Fluid Dynamics based solver has been employed to carry out an extensive investigation on the performance analysis of a thermo-syphon operating under transient conditions. There has been limited research conducted on the transient performance of thermo-syphons. This study focuses on the effects of various heat flux inputs and thermal loading conditions on the performance of a closed-loop solar hot water thermo-syphon system. The study reveals that the effect of heat flux input on heat transfer coefficient is dominant as compared to thermal loading. The results provided here can be used to optimally design thermo-syphon systems. Furthermore, it has been demonstrated that Computational Fluid Dynamics can be used as an effective tool to analyse the performance of a thermo-syphon with reasonable accuracy.

Keywords: *Computation Fluid Dynamics (CFD), Thermo-syphon, Heat Flux, Thermal Loading.*

1. INTRODUCTION

Thermo-syphon can be defined as a system that captures the solar energy through a working fluid. This occurs via natural convection, through which the

heat in the working fluid is conveyed from a solar collector (hot side) to the condenser (cooler side). Hence, there is no requirement of having an external pump for circulating the working fluid. For this reason, the thermo-syphon is considered to be a reliable and effective system to produce hot water for both the residential and industrial purposes. Soin et al., 1979 studied the effect of the insulation and liquid-level on the performance of the condenser. Furthermore, the authors also investigated the thermal performance of a thermo-syphon when the condenser contained boiling acetone and petroleum ether. The results depicted that the relationship between the efficiency of the condenser and the liquid level is linear. Subramanian et al., 2012 analysed the solar water-heating system both numerically and experimentally with identical boundary conditions. The solar water heater was designed with different header configurations. The results show that the overall thermal performance in the variable header system decreased due to the non-uniform flow in the riser tubes. Moreover, the overall thermal performance and efficiency are higher due to the uniform velocity. Yong et al., conducted experimental and numerical study investigating the effects of heat input on the heat transfer coefficient of a two-phase closed thermo-syphon. FC-72 (C6F14) has been used as the working fluid. The results show that increase in heat input leads to increased heat transfer coefficient. Esenet et al., 2005 experimentally studied three refrigerants i.e. R-134, R-407 and R-410, used as working fluids in a thermo-syphon. The three systems have been tested under the same working conditions in an attempt to determine the most effective refrigerant among the three. The results have shown that using R-410 as the working fluid is more efficient than other refrigerants, for both the loaded and non-loaded operations. Numerical analysis of modified solar condenser has been investigated by Sato et al., 2012. The authors conducted a theoretical study to analyse the effect of heat pipe tilt angle and condenser geometry on the temperature of the working fluid within the condenser, using CFD. The results established that the optimal performance tilt angle of a thermo-syphon is 45º. Many researchers have studied the effect of geometrical parameters on fluid flow properties [6, 7]. Furthermore, complex fluid flow problems have been solved using CFD based solvers with reasonable accuracy [8-13].

It can be seen from the previous review that there is limited work on combining different heat flux situations, with a wide variety of thermal loading conditions. The practical use of thermo-syphon involves a broad range of operating conditions in which the heat flux varies, coupled with many transient conditions. The present work numerically simulates the working of a thermo-syphon over a wide range of operating conditions. This is considered on the basis of day-to-day operations, and hence provides a measure of suitability of choice for effective usage.

2. NUMERICAL MODELLING

I. Geometry

Three dimensional computational geometry of a closed-loop thermo-syphon has been created for the numerical simulations. The geometry consists of several inclined copper riser pipes connected at the upper end to the upriser, and at the lower-end to the downcomer, as shown in figure 1. In the present study, the internal diameter and length of riser pipes have been chosen to be 20mm and 2000mm respectively, with a wall thickness of 0.7mm. The internal diameter of 25mm has been selected for the upriser and the downcomer, with a wall thickness of 0.7mm. This configuration is most suited for a medium range thermo-syphon. Furthermore, the diameter of the condenser is five times the diameter of the riser pipes. The thermo-syphon model has been

tilted by 53º to the horizontal, as it is equivalent to the latitude site angle of Huddersfield (UK).

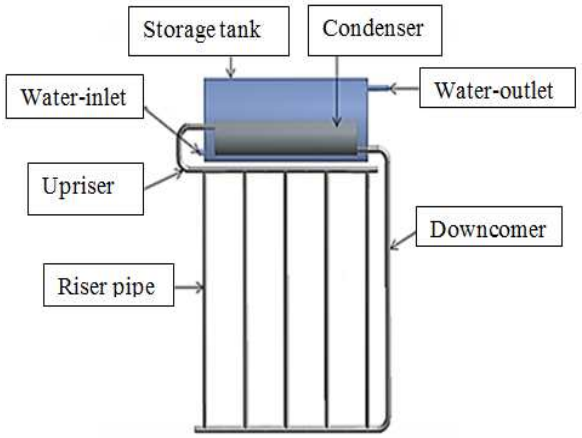

Fig. 1 Thermo-syphon Model

II. Meshing of the Flow Domain

Hybrid meshing has been employed in the present study, using both hexagonal and tetrahedral elements. Non-uniform mesh distribution has been employed, where the mesh elements are concentrated in wall proximity regions. Five layers of structured hexahedral mesh elements have been generated in the near wall regions with a growth factor of 1.2. The flow domain contains three million mesh elements, which has been previously shown by Hu et al. 2002 to describe the flow phenomena within a thermo-syphon with reasonable accuracy.

III. Boundary Conditions

Transient heat flux input and thermal loading are the two primary boundary conditions that have been used in the present study. Heat flux input to the riser pipes has been calculated using Eq. 1.

$$q = I_o\, \varepsilon\tau[\sin\delta \sin(\theta-\propto) + \cos\delta \cos(\theta-\propto)\cos\phi] \quad (1)$$

where I_o is solar radiation intensity, δ is the inclination angle, θ is tilt angle of thermo-syphon, $\propto$ is local latitude and ϕ is the hour angle, which can be calculated using equations provided by ASHRAE.

$$\varepsilon = \left[1 + 0.033\ cos\left(\frac{360N_d}{365}\right)\right] \quad (2)$$

Using the equation 2, ε which denotes the correction factor of the earth's orbit can be calculated. N_d denotes the day number, and τ denotes the atmospheric transmittance. τ value varies with location and elevation and is typically between 0 and 1, according to Sen 2008. At very high elevations with extremely clear air, τ may be as high as 0.8, while for a clear sky with high turbidity, it may be as low as 0.4.

Figure 2 depicts the variations in heat flux inputs on different days of the year, from 9am to 4pm. The three days shown cover a wide variety of seasons encountered in a solar year in Huddersfield (UK). It can be seen that during the morning period, the heat flux increases until midday, then decreases throughout the afternoon. This trend is the same for all the three days.

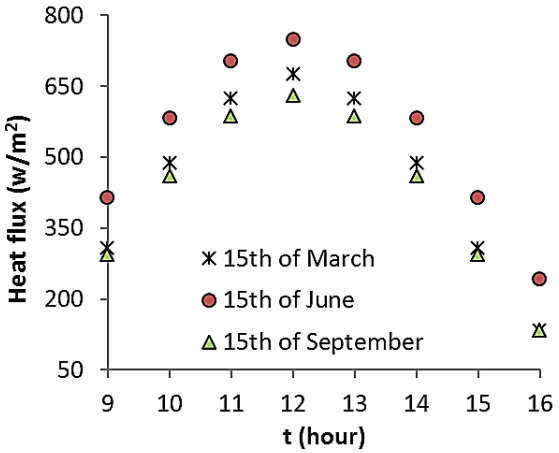

Fig. 2 Heat fluxes as a function of time for various days of the year

The data regarding thermal loading for weekdays (WD) and weekends (WE) under Danish conditions has been obtained from Lin Qin., 1998. Figure 3 depicts the variations in thermal loadings, from 9am to 4pm, over weekdays (WD) and weekends (WE). It can be clearly seen that the thermal loading is higher during the morning period as compared to the afternoon.

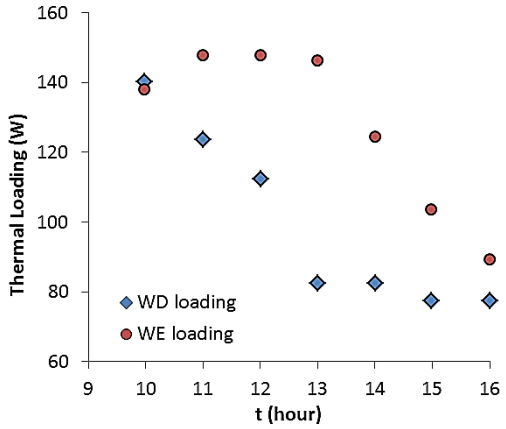

Fig. 3 Thermal loading during a weekday and weekend

IV. Solving Setting

Three dimensional Navier-Stokes equations, along-with the continuity and energy equations, have been numerically solved in an iterative manner for the transient flow of water within the thermo-syphon in the present study. Pressure Implicit Splitting of Operators algorithm for pressure–velocity coupling has been employed along-with Boussinesq approach for relative corrections in fluid's density affected by the gravitational acceleration term. Thermo-syphon model is made of copper. Second Order Upwind discretization schemes have been used for accurate flow field predictions.

3. RESULTS AND ANALYSIS

The thermo-syphon model considered in the presented study has been analysed under various transient heat flux inputs and thermal loading conditions. The following sections describe the effects of these parameters on the heat transfer coefficient, and hence on the thermo-syphon performance.

I. Effect of Heat Input variations on the Temperature Field within the Thermo-syphon

Figure 4 depicts the static temperature distribution of the working fluid within the cross-section of the middle riser pipe, for the three days of the year considered in the present study. The corresponding thermal loading condition that has been specified is that of the weekday. It can be clearly seen that the hot water occupies the near wall region that is in front of the solar rays, while the cold water settles on the other side of pipe wall. It can be clearly seen that the temperature within the riser pipe is higher on 15th June as compared to 15th March and 15th September. This means that the working fluid's temperature increases significantly on the days when the heat flux input to the thermo-syphon is higher. It is evident that more heat flux provided to the riser pipes, heats up the working fluid further. Moreover, it has been noticed that the highest temperatures attained for one hour of operation from 12 am to 1pm are 301K, 298K and 297K on 15th June, 15th March and 15th September respectively.

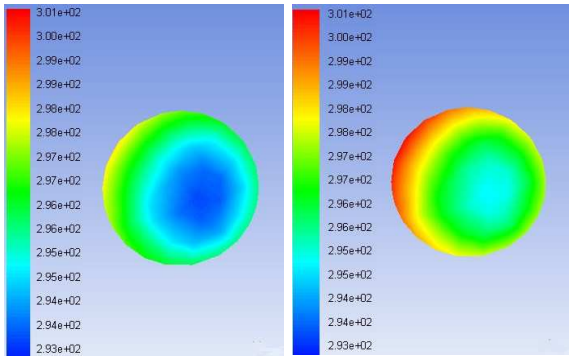

(a) (b)

Figure 5 depicts the variations in mass flow rate of the working fluid within the thermo-syphon for the same conditions as discussed above. It can be noticed that increase in heat flux input increases the mass flow rate of the working fluid. The mass flow rate of the working fluid is highest on 15th of June, as compared to on 15th of March and 15th of September.

Furthermore, it can be observed that the mass flow rate depends on the heat flux input to the thermo-syphon.

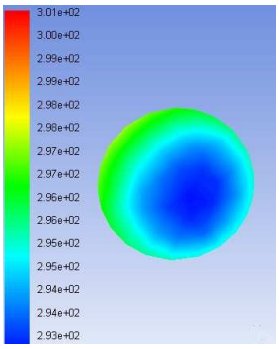

(c)

Fig. 4 Static temperature distribution within the middle riser pipe on (a) 15th March (b) 15th Jun (c) 15th September under thermal loading of the working day

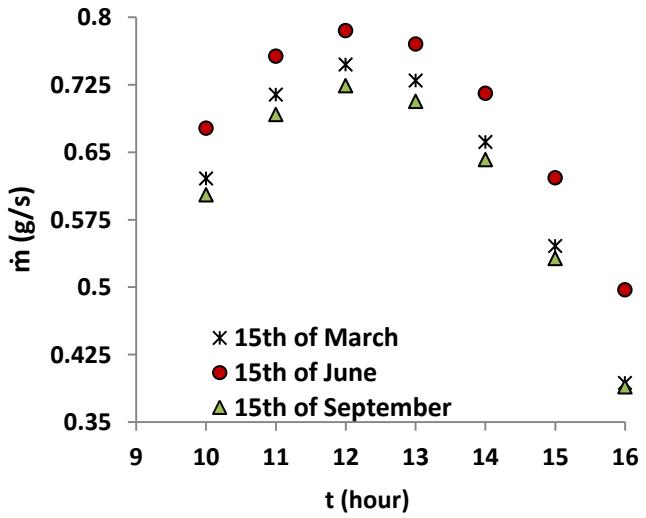

Fig. 5 Mass flow rate variations within the collector on different days of the year

Figure 6 depicts the variations of heat transfer coefficient within the cross-section of the collector for the same conditions as above. It can be clearly seen that the heat transfer coefficient within the collector is highest on 15th of June, as compared to 15th of March and 15th of September. The increase in heat flux input increases the heat transfer coefficient within the collector. Furthermore, it can be seen that the heat transfer coefficient increases, then decreases, depending on the increase and decrease in the heat flux input to the thermo-syphon.

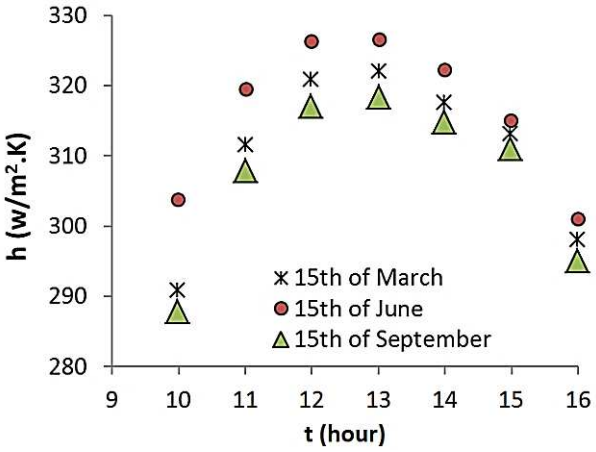

Fig. 6 Heat transfer coefficient variations within the collector on different days of the year

Figure 7 depicts the variations in the heat transfer coefficient of the working fluid within the middle riser pipe, on 15th of March, as a function of distance from the base of the riser pipe. It can be clearly seen that the heat transfer coefficient is higher at a distance of 0.5m from the base of the middle riser pipe. This means that the heat transfer coefficient decreases downstream a riser pipe. Furthermore, the heat transfer coefficient increases during the morning hours of the day, while it starts decreasing in the afternoon.

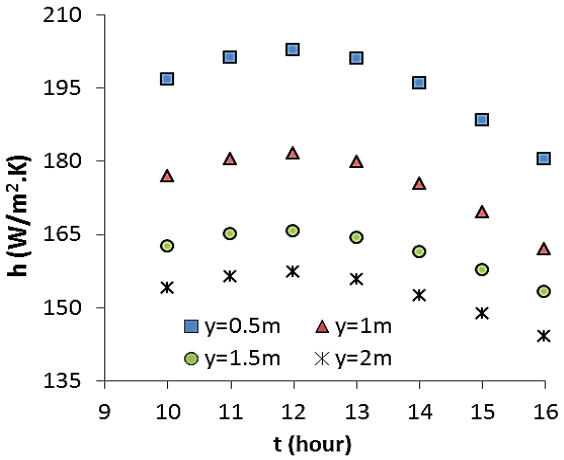

Fig. 7 Heat transfer coefficient variations at different cross-sections from the base of the middle riser pipe, on 15th of March

Figure 8 depicts the variations in the heat transfer coefficient of the working fluid within different riser pipes, at a distance of 2m from the base of the riser pipes. The data presented is for 15th of March under working day thermal loading conditions. It can be clearly seen that the heat transfer coefficient is the same on different riser pipes considered. This indicates that the heat transfer coefficient is only dependent on the heat flux input and the distance from the base of the riser pipe/s, and is independent of the location of the riser pipe in the thermo-syphon.

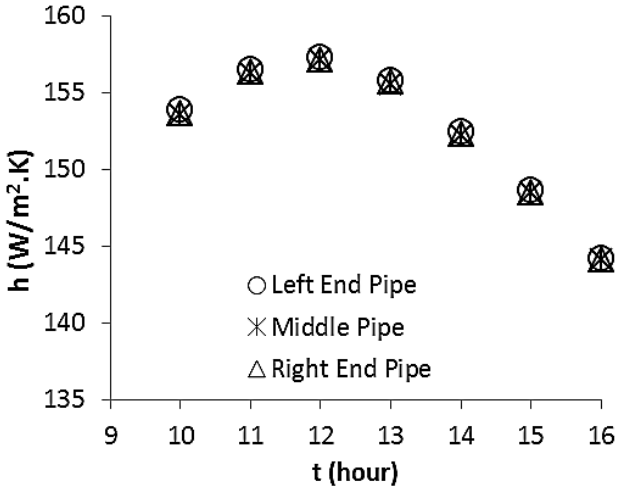

Fig. 8 Heat transfer coefficient variations within different riser pipes on 15th March, 2m from the base of the pipes

II. Effect of Thermal Loading on the Temperature Field within the Thermo-syphon

Figure 9 depicts the variation in static temperature of the working fluid within the cross-section of the middle riser pipe, for the transient thermal loading conditions considered in the present study i.e. weekday and weekend. The corresponding heat flux input is of 15th of March. It has been observed that the static temperature of the working fluid is primarily unaffected with the change in thermal loading patterns.

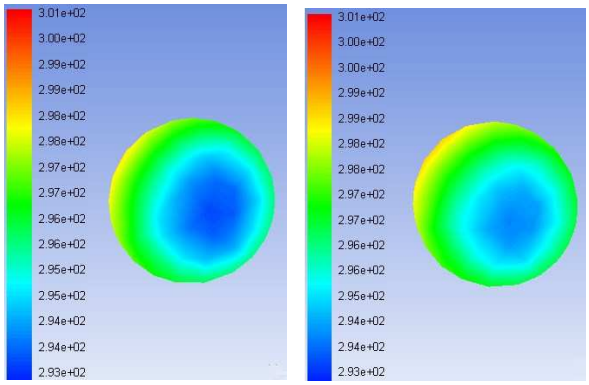

Fig. 9 Static temperature distribution within the middle riser pipe on 15th of March, under (a) weekday loading and (b) weekend loading

Figure 10 depicts the variations in mass flow rate of working fluid within the thermo-syphon, on 15th of March, for the various thermal loading considered in the present study. It can be seen clearly that the thermal loading has a small negligible effect on the mass flow rate of working fluid. Furthermore, the mass flow rate of working fluid within the thermo-syphon increases and decreases the increase and decrease in the heat flux input.

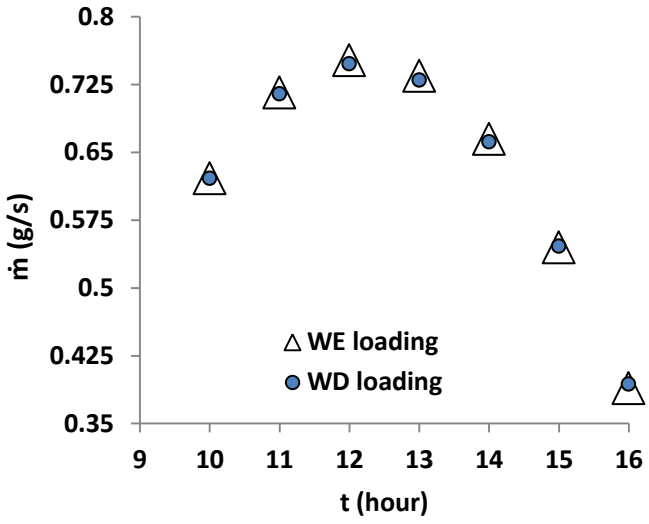

Fig. 10 Mass flow rate variations within the collector on 15th of March for various thermal loading conditions

Figure 11 depicts the variations in heat transfer coefficient within the collector, on 15th of March, for the various thermal loading considered in the present study. It can be clearly seen that the heat transfer coefficient within the collector is unaffected by thermal loading. Furthermore, it can be identified that the heat transfer coefficient increases and decreases with the increase and decrease in the heat flux input.

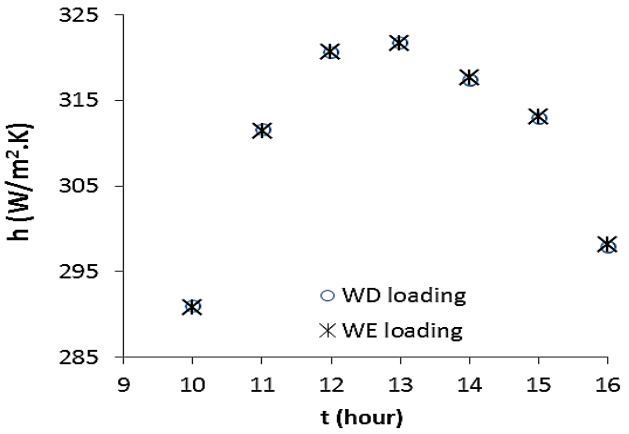

Fig. 11 Heat transfer coefficient variations within the collector on 15th of March for various thermal loading conditions

Table 1 summarises the heat transfer coefficient within the collector for various heat flux inputs and thermal loading conditions considered in the present study. This heat transfer coefficient has been calculated using the following expression:

$$h = \frac{q}{\Delta T} \quad (3)$$

where q is the heat flux input (in W/m^2) and ΔT is:

$$\Delta T = T_{wall} - T_{ref} \quad (4)$$

where T_{wall} is the area-average static temperature of the riser tubes collectively, and $T_{ref.}$ Is the reference temperature, computed as:

$$T_{ref} = \frac{T_i + T_o}{2} \quad (5)$$

where T_i and T_o are the area-average static temperatures in the cross-sections of the downcomer and upriser respectively. It can be clearly seen that the heat flux has a significant effect on thermal loading, while the thermal loading has negligibly small effect on the heat transfer coefficient.

Table1. Heat transfer coefficient for various heat flux inputs and thermal loading conditions

t (hour)	h (W/m^2.K)					
	WD March	WD June	WD Sept.	WE March	WE June	WE Sept.
10am	290.9	303.8	287.7	290.9	303.8	287.6
11am	311.5	319.3	307.8	311.4	319.3	307.7
12noon	320.7	326.3	317.0	320.6	326.3	316.9
13pm	321.8	326.7	318.3	321.7	326.6	318.2
14pm	317.5	322.2	314.7	317.6	322.3	314.7
15pm	315.1	319.1	311.2	315.1	318.9	311.3
16pm	298.2	301.3	295.4	298.1	301.4	295.4

4. CONCLUSIONS

In the present study, the effects of transient heat flux inputs and thermal loadings have been numerically investigated on the performance of a thermo-syphon. Different days of the year have been selected to cover a wide range of heat flux input, and both the weekday and weekend loading conditions have been considered. The results presented in this study suggest that the heat flux input affects the heat transfer coefficient of the thermo-syphon, whereas, the thermal loading has negligible effects. Furthermore, it has been noticed that the heat transient coefficient within the riser pipes of a thermo-syphon varies significantly downstream along these pipes; however, the location of these pipes has negligible effects on the heat transfer coefficient. This information can be used to optimise the design of thermo-syphon systems.

REFERENCES

1. R. S. Soin, K. S. Rao and D. P. Rao (1979). Performance of flat plate solar condenser with fluid undergoing phase change. *Solar Energy,* vol: 23, pp: 69 – 73.

2. J. Subramanian, S. Kumar T. Kozhndu, and T. Selvam (2012). Experimental Studies on Variable Header Solar Water Heating System. *2nd International Conference on Mechanical, Production and Automobile Engineering, 28 – 29 April, Singapore.*

3. Yong , J. P. Hwan, K. K. and Chul, J.K. (2002). Heat transfer characteristics of a two-phase closed thermo-syphon to the fill charge ratio. *International Journal of Heat and Mass Transfer*, Vol. 45, pp. 4655-4661.

4. Esen, M., &Esen, H. (2005). Experimental investigation of a two-phase closed thermosyphon solar water heater. *Solar Energy, 79*(5), 459-468.

5. Sato, A. I. Scalon, V. L. and Padilha, A. (2012). Numerical analysis of a modified evacuated tubes solar condenser. *International Conference on Renewable Energies and Power Quality, 28-30 March, Spain.*

6. Mishra, R., Singh, S. N., & Seshadri, V. (1998). Velocity measurement in solid–liquid flows using an impact probe. *Flow Measurement and Instrumentation, 8*(3), 157-165.

7. Mishra, R., Singh, S. N., & Seshadri, V. (1998). Study of wear characteristics and solid distribution in constant area and erosion-resistant long-radius pipe bends for the flow of multisized particulate slurries. *Wear, 217*(2), 297-306.

8. Palmer, E., Mishra, R., & Fieldhouse, J. (2009). An optimization study of a multiple-row pin-vented brake disc to promote brake cooling using computational fluid dynamics. Proceedings of the Institution of Mechanical Engineers, Part D: *Journal of Automobile Engineering, 223*(7), 865-875.

9. Malviya, V., Mishra, R., & Fieldhouse, J. (2009). CFD investigation of a novel fuel-saving device for articulated tractor-trailer combinations. *Engineering Applications of Computational Fluid Mechanics, 3*(4), 587-607.

10. Park, K. S., Asim, T., & Mishra, R. (2012). Computational Fluid Dynamics based Fault Simulations of a Vertical Axis Wind Turbines. *In Journal of Physics: Conference Series,* Vol. 364, No. 1, p. 012138. IOP Publishing.

11. Colley, G., & Mishra, R. (2011). Computational flow field analysis of a Vertical Axis Wind Turbine. *Renewable energy and power quality*.

12. Agarwal, V. C., & Mishra, R. (1998). Optimal design of a multi-stage capsule handling multi-phase pipeline. *International journal of pressure vessels and piping, 75*(1), 27-35.

13. Palmer, E., Mishra, R., & Fieldhouse, J. (2009). An optimization study of a multiple-row pin-vented brake disc to promote brake cooling using computational fluid dynamics. Proceedings of the Institution of Mechanical Engineers, Part D: *Journal of Automobile Engineering, 223*(7), 865-875.

14. Lin Qin (1998). Analysis, Modeling and Optimum design of Solar Domestic Hot Water Systems.

15. ASHRAE Handbook, Fundamentals, 1985.

16. Sen, Z. (2008). Solar energy fundamentals and modelling techniques (pp. 36-37). Springer.

17. Hu, J., Lee, Y. K., Blacker, T. D., & Zhu, J. (2002). Overlay Grid Based Geometry Cleanup. In IMR (pp. 313-322).